Proceedings of the Korean Nuclear Society Spring Meeting
Gyeongju, Korean, May 2003

Flooding Data Measured in Annular Narrow Gaps with Large Diameter of Curvature

J.H. Jeong
Cheonan College of Foreign Studies
Anseo-dong, Cheonan, Choongnam, 330-705 KOREA

R.J. Park, S.B. Kim
Korea Atomic Energy Research Institute
150 Dukjin-dong, Yusong-gu, Daejeon 305-353, KOREA

ABSTRACT

An experimental study on counter-current flow limitation phenomena in narrow annular passages was carried out. The gap sizes examined were 1, 2, 3 and 5 mm. This is very small compared with the outer diameter of the annular passage, 500 mm. It was visually observed that a CCFL might occur in some part of the periphery while the other part is remained at a counter current flow regime. That is, non-uniform behaviours of fluids due to a 2-dimensional effect appear in a large diameter facility. Because of this non-uniformity, a CCFL is defined in the present work as the situation where net water accumulation is sustained. No amount of provided water should be allowed to penetrate the gap and should accumulate over the gap at CCFL criterion. The measured data are presented in the form of Wallis' type correlation. The data fit well when the average circumference is used as the characteristic length scale of the Wallis parameter. It was found that the effects of gap size diminishes when the radius of curvature of the annular passage become large.

1. INTRODUCTION

Counter-current flow configuration between two separate fluids is widely used in industries such as power plants and chemical process plants using fluids to achieve their functions. This is because this flow configuration gives maximum efficiency in heat and/or mass transfer between two phases. This flow structure is not able to be preserved by a limiting phenomenon known as counter-current flow limitation (CCFL) or flooding. If either liquid or gas flow is supplied more than this criterion, the flow pattern changes to a chaotic flow regime from stable counter-current flow and the fluids flow co-currently in the direction of the gas flow. In consequence, the liquid phase is not able to reach the plenum where the gas phase comes out. The CCFL phenomenon has been of interest of chemical engineers since 1930s because of its importance in designing unit process or facility. This phenomenon has also been of importance in the field of nuclear power plant (NPP) safety analysis (Mayinger et al. 1993, Chun and Park, 1985, Jeong et al. 1998).

Table 1. Previous investigations on CCFL in rectangular passage

Author	W (cm)	S (cm)	L (cm)	Correlation	CL.
Cheng (1990)	NA	NA	NA	$j_G^{*2}[W^{*2} j_G^{*2} + 150 + \frac{2W}{S}] + j_L^{*2}\left[(W^{*2} j_G^{*2} + 150)\frac{W^{*4} j_G^{*4}}{4}\frac{\rho_G}{\rho_L}\frac{W^{*6} j_G^{*6}}{4}\right] +$ $j_G^{*}\left|j_L^{*}\right|\left[W^{*2} j_G^{*2}(W^{*2} j_G^{*2} + 150)\sqrt{\frac{\rho_G}{\rho_L}}\right] = \frac{2}{3C_f}$, $W^{*} = 2W/\lambda$, $\lambda = \sqrt{\sigma/(g\Delta\rho)}$	2W
Celata et al. (1985)	15.0	0.2 0.5 1.0	30 12	$j_G^{*1/2} + j_L^{*1/2} = 0.82$, $K_G^{*1/2} + 1.6K_L^{*1/2} = 1.2$	S
Osakabe & Kawasaki (1989)	10.0	0.2 0.5 1.0	123.5	$j_G^{*1/2} + 0.8 j_L^{*1/2} = 0.58$	W
Lee (1993)	NA	NA	NA	$j_G^{*1/2} + m j_L^{*1/2} = C$, * $m = 0.5194 + 3.4019\left(\frac{S}{W}\right)$, $C = 0.6959 + 0.1618\log_{10}\left(\frac{S}{W}\right)$	2W
Sudo & Kaminaga (1989)	3.3 6.6	0.23 0.53 0.83 1.23	7.2 36.2 78.2	$j_G^{*1/2} + m j_L^{*1/2} = C$, $m = 0.5 + 0.0015Bo^{1.3}$, $C = 0.66\left(\frac{S}{W}\right)^{-0.25}$, $Bo = \frac{W \cdot S(\rho_L - \rho_G)g}{\sigma}$	S
Ruggles (1990)	8.4	0.127	61.0	$j_G^{*1/2} + 0.67 j_L^{*1/2} = 0.50$	W
Mishima (1984)	4	0.15 0.24 0.50	47.0	$j_G^{*1/2} + j_L^{*1/2} = 0.6$	2W

CL. characteristic length, W : span, S : gap size, L : length
* obtained by regression analysis for Mishima (1984), Osakabe & Kawasaki (1989) and Sudo & Kaminaga (1989)'s experimental data

Table 2. Previous investigations on CCFL in annular passage

Author	O.D. (cm)	I.D. (cm)	L (cm)	S (cm)	Correlation	CL.
Richter (1981)	NA	NA	NA	NA	$C_w N_B^{'3} j_G^{*6} S^{*2} j_L^{*2} + C_w N_B^{'} j_G^{*4} + 150 C_w \frac{j_G^{*2}}{S^*} = 1$	W
McQuillan et al. (1985)	6.0	3.8	27.8	1.1	$\frac{\zeta\sigma(D_a^2 - D_r^2)}{4h^3} - \rho_L g\left(\frac{\pi D_r}{2} + \frac{4h}{3}\right) + \frac{f_w \rho_L D_r}{h}\left(\frac{A}{A - A_l}\right)^2 V_L^2 = 0,$ $\sigma\zeta = h\Delta P$	NA
Ueda, Suzuki (1978)	2.8 3.5 4.0	1.0	100	0.9 1.25 1.5	$Fr = 8.29\log_{10} X + 19.18$, $Fr = \sqrt{\frac{\rho_g (u_G + u_L)^2}{\rho_L g y_i}}$, $X = \left(\frac{1}{\mathrm{Re}_L}\right)^{1/3}\left(\frac{\rho_L g D_{eq}^2}{\sigma'}\right)^{1/4}\left(\frac{\eta_G}{\eta_L}\right)^{2/3}$	NA
Roesler, Groll (1991)	4.9	3.9	137	0.5	$2B_4 f_i \delta^5 (5 f_i + \delta f_i^{'})(B_1^2 - 4B_4\delta^5 f_i)^{-1/2} +$ $(2 f_i + \delta f_i^{'})[B_1 + (B_1^2 - 4B_4\delta^5 f_i)^{1/2}] = 0$ $B_1 = \frac{1}{\Delta h_G \rho_L \pi d_i}$, $B_4 = -\frac{\rho_L g}{3\rho_G \eta_L^2}\left(\frac{2}{\Delta h_G \pi d_i^2}\right)^2$	NA
Glaeser (1992)	479	429	664	25.0	$K_G^{*1/2}\sqrt{\frac{\nu_G^{2/3}}{g^{1/3} l}} + 0.011 K_L^{*1/2} = 0.0245$, $l = 0.5\pi d_{outer} \sin^2(0.5\theta_{ECC-BCL})$	NA
Ragland et al. (1989)	10.16	9.064	94.5	0.546	$j_G^{*1/2} + 0.88 j_L^{*1/2} = 1.0$	D_h
Richter et al. (1979) *	44.45	39.37 34.29	--	2.54 5.08	$j_G^{*1/2} + 0.8 j_L^{*1/2} = 0.38$ *	D_h W
Koizumi et al. (1997)	10.0	9.9 9.8 9.6 9.0	50.0	0.05 0.1 0.2 0.5	$j_G^{*1/2} + 0.23 j_L^{*1/2} = 0.32$ for 2 mm gap ** $j_G^{*1/2} + 0.35 j_L^{*1/2} = 0.35$ for 1 mm gap **	D_h
Nakamura et al. (1990)	22.0	20.0	--	1.0	$j_G^{*1/2} + 0.78 j_L^{*1/2} = 0.37$ ***	W
Mishima (1984)	NA	NA	NA	NA	$j_G^* - \frac{\varepsilon}{1-\varepsilon}\sqrt{\frac{\rho_G}{\rho_L}} j_L^* = \sqrt{\frac{\varepsilon^3(1-\varepsilon)}{3 f_i}\left[1 + \frac{3 f_{wL} j_L^* \lvert j_L^* \rvert}{(1-\varepsilon)^3}\right]}$	2S

CL. : characteristic length, W : average circumference, S : gap size, D_h : hydraulic diameter(=2S), L : length
* Richter et al. presented their measurements in terms of Wallis parameters using hydraulic diameter (D_h) as a CL and later Osakabe & Kawasaki (1989) correlated them in terms of Wallis parameters using W as a CL
** original data were presented in terms of Wallis parameters and correlated by Jeong et al. (1998)
*** original data were presented in terms of Wallis parameters and correlated by Osakabe & Futamata (1996)

In previous literature, the CCFL phenomena in annular and rectangular gap geometries have been investigated in order to analyze the NPP's emergency core cooling water bypass (Mayinger et al. 1993), direct-vessel injection (DVI) (Lee at al. 1995) and safety margin of a research reactor's rectangular fuels (Cheng 1990, Mishima & Nishihara 1985, Sudo & Kaminaga 1989). Most analytical models and measured data on CCFL have been presented in terms of the Wallis parameter (j_k^*) or Kutateladze number (K_k^*) defined as follows:

$$j_k^* = j_k \sqrt{\frac{\rho_k}{gD(\rho_L - \rho_G)}} \quad (1)$$

$$K_k^* = j_k \sqrt[4]{\frac{\rho_k^2}{g\sigma(\rho_L - \rho_G)}} \quad (2)$$

Where, D, g, ρ, and σ represent diameter as a characteristic length, gravitational acceleration, density, and surface tension. The principal difference between these two dimensionless numbers is the choice of characteristic length. Wallis' parameter uses test section geometry such as diameter, gap width and span while the Kutateladze number uses Taylor wave length. Due to this fact, the Kutateladze number seems to be more adequate in describing instability-induced phenomena such as CCFL. However, Wallis' parameter is still widely used by many investigators. When Wallis' parameter is selected to describe CCFL models and fit their measurements, investigators have to make a decision on what length scale to use. If the geometry of the test section is far from the circular pipe, there is no general guidance for the selection. Table 1 and 2 list up previous CCFL investigations performed with rectangular and annular passages, respectively. The tables show the geometries of experimental facility as well as the suggested correlations. In addition, the characteristic length scales used for Wallis parameter is shown if applicable. For rectangular channels, various characteristic lengths have been used depending on the authors to correlate their measurements. Sudo & Kaminaga (1989) and Celata et al. (1985) used the gap width, S, while Osakabe & Kawasaki (1989) and Ruggles (1990) used the span, W, as the characteristic length. Furthermore, Cheng (1990), Mishima (1984) and Lee (1993) suggested twice the span (2W) as the characteristic length scale. A similar situation happens with annular passages as well. Richter et al. (1979), Koizumi et al. (1997), Ragland et al. (1989) and Lee et al. (1995) used hydraulic diameter, which is the same as twice the gap size (2S) for annular passages, while Richter (1981), Osakabe & Kawasaki (1989) and Nakamura et al. (1990) used the average circumference of the annular passage as the characteristic length scale. In addition, there was a study that substitutes another characteristic length scale for the original one. Richter et al. (1979) measured CCFL points using vertical annulus gap geometry whose gap size is 1 and 2 inches. They presented their measurements in terms of Wallis' parameters using hydraulic diameter (D_h = 2S) as a characteristic length scale. Later, these data have been correlated by Osakebe & Kawasaki (1989) in terms of Wallis' parameter using average circumference (W) as a characteristic length scale as follows:

$$j_G^{*1/2} + 0.8\, j_L^{*1/2} = 0.38. \quad (3)$$

It seems that many authors picked their characteristic length scale not based on physical reasoning but based on the best fit of data during the course of data regression. In the meantime, Mishima (1984) derived an analytical CCFL correlation and suggested two times the gap size should be used. In the present study, the selection of length measure for the characteristic length in Wallis parameter will be examined.

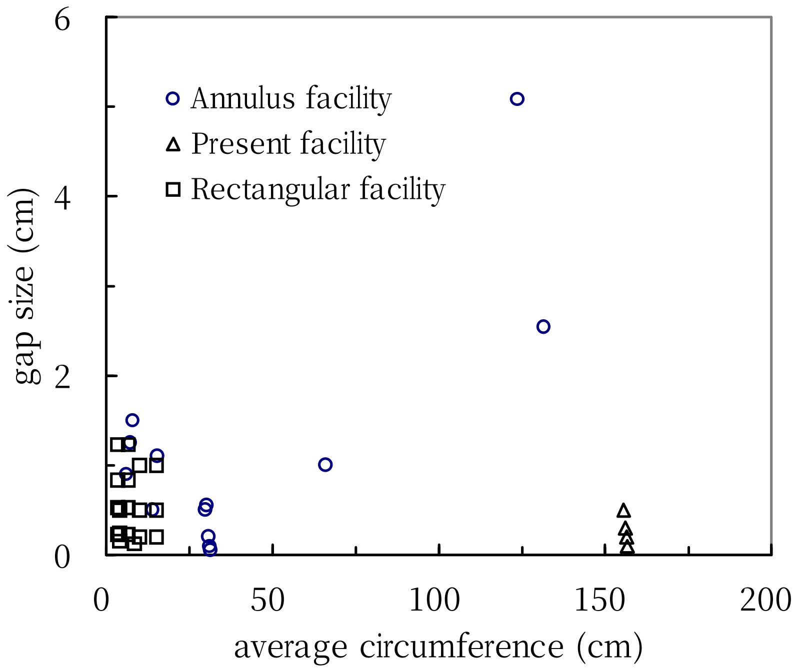

Figure 1. Geometries of CCFL test facility of which passages are narrow gaps

The geometric scales of the experimental facilities listed in tables 1 and 2 are compared in fig. 1. The Glaeser (1992)'s facility is not compared in this plot since it is much larger than the others. Glaeser (1992)'s facility known as the UPTF is real nuclear reactor scale. The average circumference stands for span of rectangular passages and the circumference of the middle between inner and outer walls of annular passages. Most previous CCFL experiments in annular passages were performed with small diameter (small average circumference) test sections. Furthermore, gap sizes of most of them were large. An outer diameter of the annular passage smaller than 10 cm and gap sizes around 10 mm are dominant in previous investigators' experiments. If a counter current flow is developed in the test sections of this size, the hydrodynamic phenomena would be quite uniform over the whole periphery while the phenomena may show a 3-D effect in actual or large size test sections. Figure 1 also shows the geometries of the present facility. Compared with the previous experimental facilities, the diameter of the present facility is large and the gap size is small. That is, the gap size to average circumference ratio of the present facility is much smaller than the previous ones. Koizumi et al. (1997) carried out an experimental study on CCFL in narrow annular passages. They measured flooding velocities in gap sizes ranging from 0.5 to 5 mm, which is nearly the same as the present gap size. However, the outer diameter of annular passages was 10 cm, which is much smaller than the present one.

The effect of test section diameter associated with characteristic length scale in dimensionless numbers is not well understood so far. In this regard, it is necessary to carry out CCFL experiments in narrow annular passages with a large radius of curvature and have a visual observation on what is happening in a large diameter test section. The objectives of the present experiments are to visually observe the two-phase flow behaviour inside a narrow annular gap and investigate the gap size effect on CCFL under large diameter conditions.

2. EXPERIMENTAL FACILITY

A schematic diagram of the test facility is shown in Fig. 2. The test rig consists of a test section, a water reservoir, an air buffer tank, pumps & valves, pressure transducers, thermocouples and turbine flow meters. Distilled water and air are used as working fluids. The high-pressure air coming out of the building supply line is provided to the flow control valve and turbine flow meter via an air filter and an air buffer tank whose volume is 1.3 cubic meters. The air buffer tank is used in order to damp down air pressure fluctuation and make a smooth change of air flow. The metered air is introduced to the lower plenum of the test section and goes up through a multi-holed plate that is used to achieve an evenly distributed flow velocity. The water in the reservoir is forced to flow by a controllable DC pump and the flow-rate is measured by a turbine flow meter. The water is supplied to the upper part of the test section through holes made on the central pole. The central pole plays the roles of water supply line as well as alignment axis for the test section. The water coming down to the lower plenum returns to the water reservoir by a pump. The water circulates in a closed loop and the air is discharged into the atmosphere. A cooling coil is installed inside the water reservoir to maintain the water temperature at a constant level. The cooling coil gets rid of the heat generated by pumping work. Measurements are made on the differential pressure across the test section, system pressure, air-line pressure, air flow rate, and supplied water flow rates. All signals coming out of the sensors are read by an HP-VXI data acquisition system and graphically displayed on a PC-monitor as well as saved on a hard-disk.

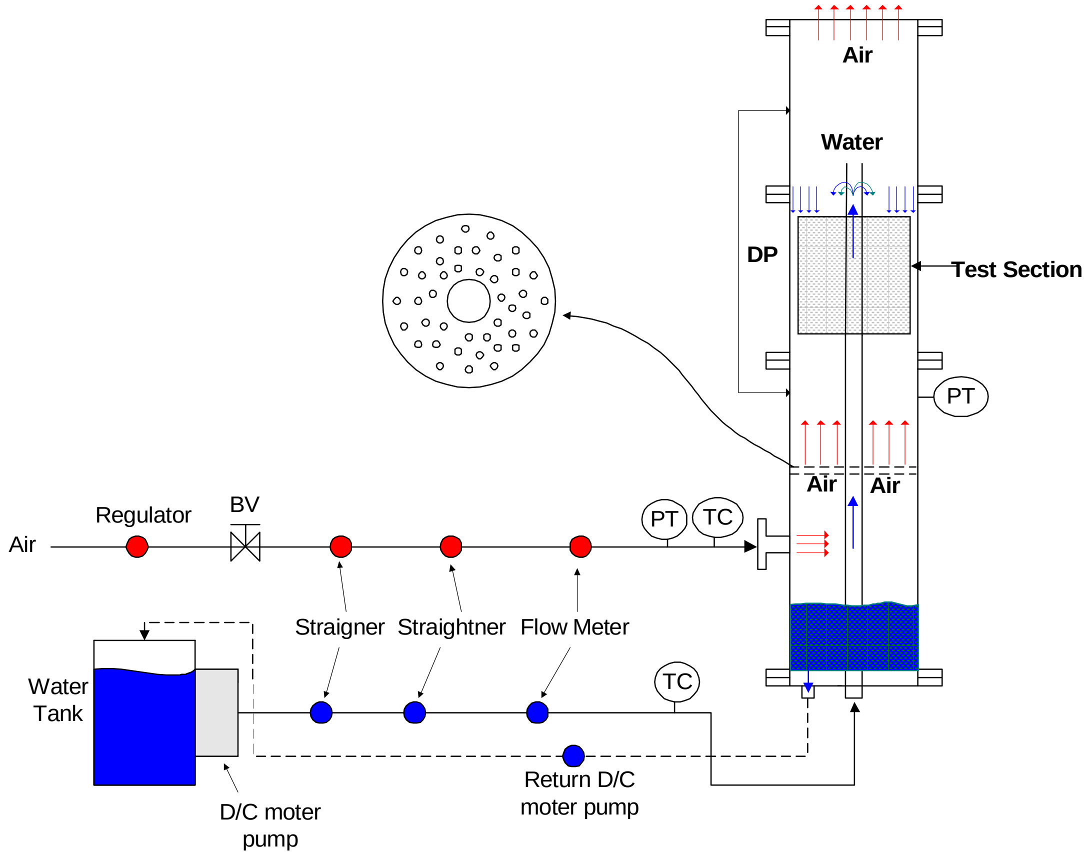

Figure 2. Schematic diagram of the experimental facility

The parts of the test section are made of acrylic resin to allow the visual observation on the two-phase flow behaviour inside the gaps. The inner diameter of the outer pipe making annular passage and the length of the inner cylinder are 500 and 250 mm, respectively. Gap sizes of 1, 2, 3 and 5 mm were made by changing the inner cylinders to various diameters. Even though most of parts of the test section were machined by a CNC lathe, the gap sizes were not so uniform due to manufacturing tolerance. For instance, a gap size of 1 mm is too small compared with the diameter of the outer pipe of 500 mm. A manufacturing tolerance of 0.1% causes the deviation of ±0.25 mm in the gap size, which corresponds to 25% variation for a 1 mm gap.

3. PROCEDURES AND CCFL DEFINITION

Each run starts with a regulation of the water flow rate at a pre-determined level. The air flow-rate is step-wisely increased from nil. At each level of air flow-rate, the two-phase flow behaviour inside a gap and water accumulation in the upper plenum are observed with the naked eye. The pressure difference between the top and the bottom of a gap is monitored as well. Both air and water flow-rates are not altered and observed for more than 10 minutes. If there is no sign of water accumulation in the upper plenum, the air flow-rate is increased further. This process is repeated until there is a significant increase in the differential pressure across the gap and water starts to accumulate in the upper plenum. These two signs, water accumulation and a significant increase in the differential pressure, are used as an experimental definition of the occurrence of CCFL in the present study. This definition has been generally accepted in previous literature. Even if CCFL may locally occur in a part of the gap, the point where there is no water accumulation in the upper plenum is not considered as the CCFL. This is because such a condition does not cause a problem from the viewpoint of nuclear safety analysis. At any rate, all the supplied water penetrates gaps and reaches the lower plenum. Further details on observations are in the section below.

4. RESULTS AND DISCUSSIONS

4.1 Visual Observations

Each run starts with fixing a liquid phase flow rate at a pre-determined value. Air flow-rate is stepwise increased from zero while the liquid flow rate is fixed at a set-value. The pressure difference between the top and the bottom of an annular gap is monitored. In addition, the behaviours of water and air inside a narrow annular gap are visually observed and the images are captured using a camera. Figure 3 shows a trace of the differential pressure for the test section whose gap size is 1 mm. The water supply is fixed at $j_L^{*1/2}$=1.152. A somewhat long trace before time zero in Fig. 3 was truncated to give a clear figure around the onset of CCFL. The trace can be divided into three regions. Region I covers up to 800 seconds in Fig. 3. A dozen stepwise increases in air flow-rate were made before 800 seconds. Through this period, the water supplied to the upper plenum penetrates the annular gap so that no accumulation of water is observed in the upper-plenum. The pressure difference across the annular passage fluctuates within a limited range. Region II extends from the end of region I to 1200 seconds. The air flow rate increased slightly at 800 seconds. The water supplied into the upper-plenum started to accumulate. Water accumulation does not continue over a couple of minutes but penetrates the gap until no accumulated water remains in the upper-plenum. After around a minute, the water starts to accumulate again. That is, the water in the upper plenum shows cyclic behaviour of accumulation and penetration. This cyclic behaviour continues until the air flow rate increases up to just below the value of CCFL. Through this region, the pressure difference between the top and the bottom of the annular passage increases and drops in accordance with the cyclic behaviour of the water. The pressure difference increases when water accumulates and decreases when the water penetrates. However, if air flow increases just slightly more than that of the CCFL criterion, the water accumulation continues and never shows a cyclic behaviour. This is region III. The average pressure difference continues to increase as far as the accumulation height increases in this region.

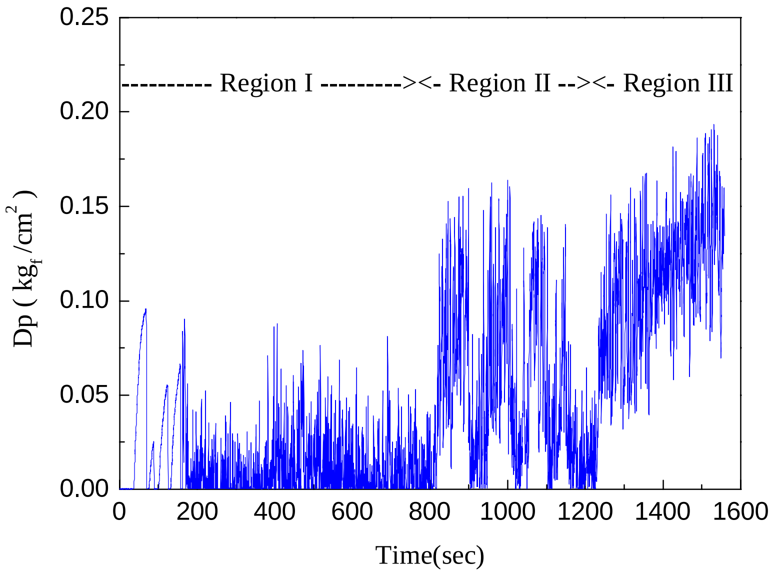

Figure 3. Pressure difference between the top and the bottom of a 1 mm wide annular passage ($j_L^{*1/2}$=1.152)

It was visually observed that the flow behaviour inside gaps is not uniform, as can be seen in Fig. 4. This photograph shows typical flow behaviour in region II. When the air flow is increased up to region II, CCFL initiates at the top of the annular gap. However, the region where CCFL occurs is limited in width. That is to say, some part of the annular gap is under CCFL conditions and other parts remain at a counter-current flow pattern. This means that water is prevented from penetrating at some part of the gap while allowed to flow downwards at other parts. The CCFL limited region expands with an increase in the air flow rate. Through a set of experimental runs, it was observed that the part of the gap where CCFL initiates was always the same. The reason is believed to be the manufacturing tolerance of the rig. The parts of the test section are made of acrylic resin to allow visual observation on the two-phase flow behaviour inside gaps. The thick resin pipe was machined by a CNC lathe to make the parts of the test section. A machining tolerance of ±0.1 % produces a variation of ±0.25 mm in gap size for the present test section the diameter of which is 500 mm. The intended gap size of 1 mm may vary from 0.75 to 1.25 mm, which corresponds to ±25 % deviation. For a 2 mm gap, the deviation could be 12.5 %. It is a large deviation in comparison with the gap size of 1 mm. In spite of the fact that water can not penetrate the gap at some part of the periphery due to local CCFL, this air velocity is not defined as the CCFL gas velocity. This is because all the water supplied to the upper plenum penetrates the gap anyway and goes to the lower plenum through the other part of the gap.

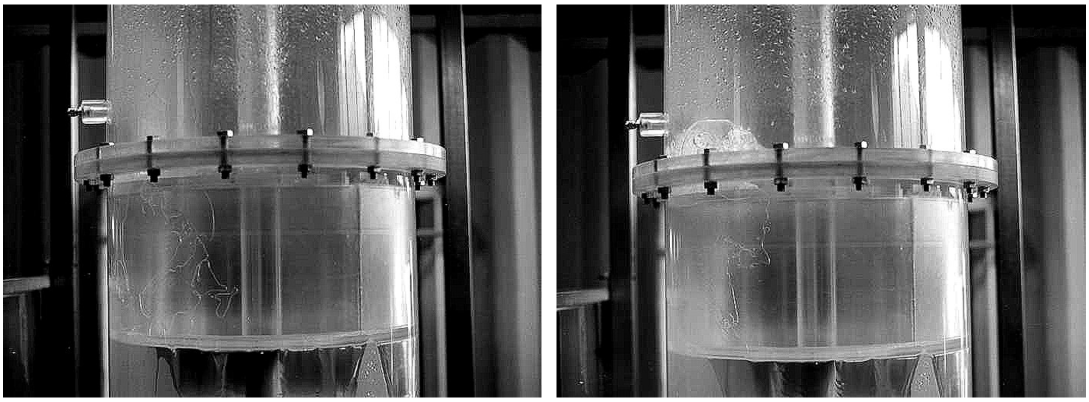

(a) (b)

Figure 4. Partially limiting CCFL (1 mm gap, $j_L^{*1/2}$=1.152)

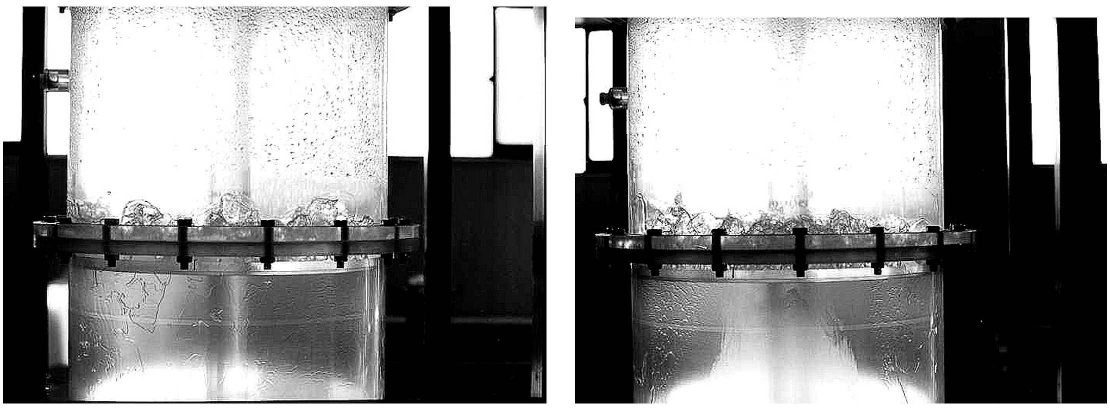

(a) (b)

Figure 5. Fully limiting CCFL (1 mm gap, $j_L^{*1/2}$=1.152)

If air flow rate is increased further, the flow configuration goes to region III. At this air flow rate, the whole periphery is controlled by CCFL as shown in Fig. 5(a). Sometimes, however, accumulated water penetrates through a part of the gap as shown in Fig. 5(b). This penetration lasts for a while and ends. Even though temporary penetration happens, water accumulation in the upper-plenum still continues. Based on these observations, the CCFL is defined in the present work as the situation where net water accumulation is sustained. It was found that the air velocities for CCFL are around 15% larger than those for the initiation of region II.

4.2 CCFL measurements

Figure 6 shows the present measurements for 1, 2, 3 and 5 mm gaps in terms of Wallis' parameter. The gap size (S) is used as the characteristic length scale in this plot. Gap sizes of the present facility, 1, 2, 3 and 5 mm, are less than the wavelength of Taylor instability, 17.2 mm, as defined by $\lambda_T = 2\pi\sqrt{\sigma / g\Delta\rho}$. The average circumference of the present facility, around 1570 mm, is much larger than the Taylor wavelength. The ratio of gap size to average circumference is around 0.4 ~ 2 % for the present facility. Compared with the gap size, the circumferential length is so much large that it can be assumed to be infinite. Therefore, the average circumference may not be appropriate to play a role of characteristic length scale for taking the effect of gap size into account. In this regard, measurements plotted in Fig. 6 are expressed in terms of Wallis' parameters with characteristic length scale of gap size. Richter et al. (1979) and Koizumi et al. (1997)'s measurements are plotted as well in this plot. Hydraulic diameter (D_h) was used to present their measurements as a characteristic length scale in the original literatures by both of investigators. Richter et al.'s (1979) test section consists of 17.5 in (44.45 cm) diametered outer pipe and 15.5 in (39.37 cm) and 13.5 in (34.29 cm) diametered inner pipes to produce 1 in (2.54 cm) and 2 in (5.08 cm) gaps. The outer diameter of the Richter et al.'s test section is close to the present one, 500 mm. In terms of gap size, however, it can be said that the present test section is much smaller than that of Richter et al.. The gap sizes of the Koizumi et al. (1997)'s test section varies from 0.05 mm to 0.5 mm, which are nearly the same as the gap size of the present test section. However, the outer diameter of the annular passage of the Koizumi et al. (1997)'s test section is 10 cm, which is much smaller than the present one. Fig. 6 shows no general tendency in variation depending on gap size. The present data are several folds larger than Koizumi et al.'s data even though the gap sizes are nearly the same. On the contrary, Richter et al.'s data are closer to the present data in spite of large discrepancy in gap size.

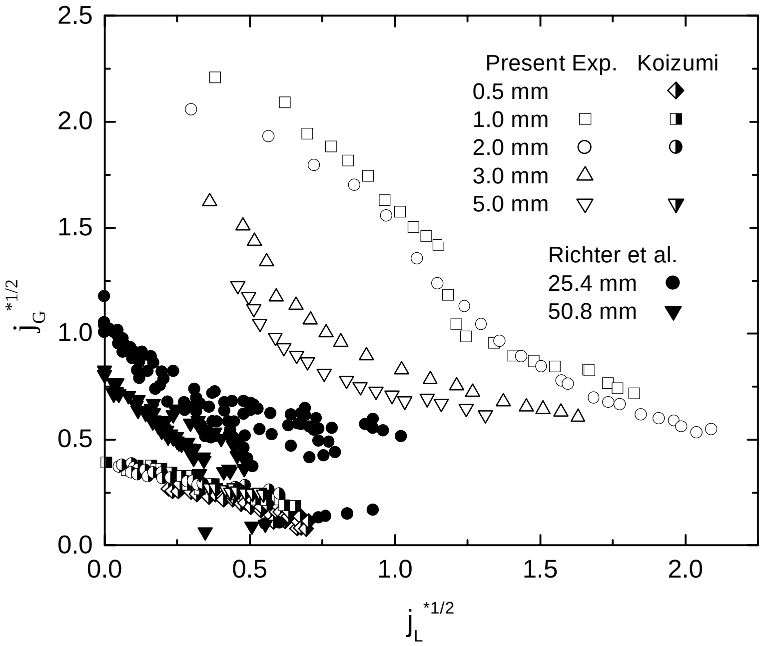

Figure 6. CCFL points in Wallis' parameter with gap size (= D_h /2) as characteristic length

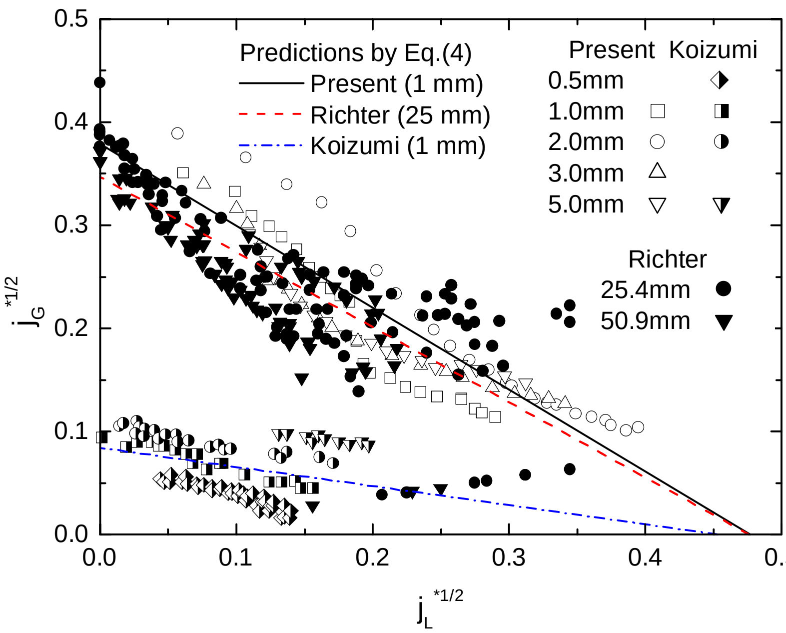

Figure 7. CCFL points in Wallis' parameter with average circumference as characteristic length

All data presented in Fig. 6 are transformed into Wallis parameter using average circumference as the characteristic length scale and plotted in Fig. 7. Richter et al.'s data appears to be slightly smaller than the present data even though the difference in gap size is large. Koizumi et al.'s data appears to lie farther even if there is little difference in gap size. However, these three data sets are laid in order of average circumference. The average circumference of the present data, Richter et al.' data, and Koizumi et al.'s data are 156.8~155.5, 131.7~123.7, and 31.3~29.8 cm, respectively. The average circumference of Richter et al. and Koizumi et al.'s facility corresponds to 84 % and 20 % of the present test facility. Figure 6 and 7 show that average circumference seems to be more appropriate than the gap size or hydraulic diameter to present or correlate the CCFL data gathered using annular passages. However, there still leaves a difficulty to generalize this statement. Koizumi et al.'s data become scattered in Fig. 7, while they flock together on a line in Fig. 6. In other words, Koizumi et al.'s data show better agreement when expressed in terms of Wallis parameter using gap size as a characteristic length scale than using average circumference.

The measurements shown in Fig. 7 are correlated in the form of Eq. (4).

$$j_G^{*1/2} + m\, j_L^{*1/2} = C \tag{4}$$

where, $j_k^* = j_k \sqrt{\dfrac{\rho_k}{gW(\rho_L - \rho_G)}}$.

As stated above, the average circumference is used as the characteristic length scale. In order to take advantage of it in determining the constants m and C, a ratio of average circumference to the Taylor wavelength is considered. This ratio reduces to a bond number, N_B, whose relation is as follows:

$$\frac{W}{\lambda_T} = \sqrt{\frac{W^2 g \Delta\rho}{\sigma}} = \sqrt{N_B} \quad . \tag{5}$$

The constants m and C are fitted by the least-square method as follows:

$$m = -1.60 + 0.43 \log_{10} N_B \tag{6}$$

$$C = -0.78 + 0.21 \log_{10} N_B \quad . \tag{7}$$

These expressions show that the constants *m* and *C* increases with an increase in average circumference. The predictions by Eq. (4) for the present, Richter et al.'s, and Koizumi et al.'s data are displayed in Fig. 7. This plot shows a good agreement between measured data and Eq. (4) through (7).

5. CONCLUDING REMARKS

Counter current flow limitation in narrow annular passages having large diameter of curvature has been investigated. A principal difference between the present facility and the previous facilities providing annular passage is the small gap size compared with the radius of curvature. The gap sizes tested were 1, 2, 3 and 5 mm. This is very small compared with the outer diameter of the annular passage, 500 mm. It was visually observed that a CCFL might locally occur in some part of the periphery while the other parts remain at the counter current flow regime. In spite of the fact that water can not penetrate the gap at some part of the periphery due to local CCFL, this air velocity is not defined as the CCFL gas velocity. This is because the water supplied to the upper plenum penetrates the gap and goes down to the lower plenum through another part of the gap. Based on these observations, CCFL is defined in the present work as the situation where net water accumulation is sustained. That is, no amount of supplied water should be allowed to penetrate the gap and accumulate over the gap at the CCFL criterion. Comparison among the present and previous experimental data show that average circumference is more appropriate than the gap size or hydraulic diameter to correlate the CCFL data obtained from annular passages having large diameter regardless of gap size. An empirical correlation in terms of Wallis' parameter was developed by means of the least-squares method from the measured data. The average circumference was used as the characteristic length and the results show that the absolute value of slope and the y-intercept of the Wallis type CCFL correlation increase with an increase in average circumference.

REFERENCES

1. Celata, G.P., Farello, G.E., Furrer, M., Cumo, M. 1985 Flooding experiments in a rectangular geometry, ENEA, RT/TERM/85/3.
2. Cheng, L.Y. 1990 Counter-current flow limitation in thin rectangular channels, BNL Report, BNL-44836.
3. Chun, M.H., Park, J.W. 1985 Filmwise reflux condensation length and flooding phenomena in vertical U-tubes, *J. of Korean Nuclear Society* **17**, 45-52.

4. Glaeser, H. 1992 Downcomer and tie plate countercurrent flow in the upper plenum test facility (UPTF), *Nucl. Eng. & Des.* **133**, 259-283.
5. Jeong, J.H., Park, R.J., Kim, S.B. 1998 Thermal-hydraulic phenomena relevant to global dryout in a hemispherical narrow gap, *Heat and Mass Transfer* **34**, 321-328.
6. Koizumi, Y., Nishida, H., Ohtake, H., Miyashita, T. 1997 Gravitational water penetration into narrow-gap annular flow passages with upward gas flow, *Proceedings of NURETH-8*, Volume 1, 48-52.
7. Lee, S.Y. 1993 A new flooding correlation development and its critical heat flux predictions under low air-water flow conditions in Savannah River site assembly channels, *Nuclear Technology* 104, 64-75.
8. Lee, S.C., Mo, C., Nam, S.C., Lee, J.Y. 1995 Thermal-hydraulic behaviours and flooding of ECC in DVI systems, KAERI Report, KAERI/CM-045/95.
9. Mayinger, F., Weiss, P., Wolfert, K. 1993 Two-phase flow phenomena in full-scale reactor geometry, *Nuclear Engineering and Design* **145**, 47-61.
10. Mishima, K. 1984 Boiling burnout at low flow rate and low pressure conditions, Ph.D. Thesis, Research Reactor Inst., Kyoto Univ..
11. Mishima, K., Nishihara, H. 1985 The effect of flow direction and magnitude on CHF for low pressure water in thin rectangular channels, *Nuclear Engineering and Design* **86**, 165-181.
12. Nakamura, H., Koizumi, Y., Anoda, Y., Tasaka, K. 1990 Air-water two-phase flow in large vertical annuli, *Proceedings of 27th National Heat Transfer Symposium of Japan*, 964-966 (in Japanese).
13. Osakabe, M., Kawasaki, Y. 1989 Top flooding in thin rectangular and annular passages, *Int. J. Multiphase Flow* **15**, 747-754.
14. Ragland, W.A., Minkowycz, W.J., France, D.M. 1989 Single- and double-wall flooding of two-phase flow in an annulus, *Int. J. Heat and Fluid Flow* **10(2)**, 103-109.
15. Rempe, J.L., Wolf, J.R., Chavez, S.A., Condie, K.G., Hagrman, D.L., Carmack, W.J. 1994 Investigation of the coolability of a continuous mass of relocated debris to a water-filled lower plenum, EG&G Idaho Report, EGG-RAAM-11145.
16. Richter, H.J. 1981 Flooding in tubes and annuli, *Int. J. Multiphase Flow* **7**, 647-658.
17. Richter, H.J., Wallis, G.B., Speers, M.S. 1979 Effect of scale on two-phase countercurrent flow flooding, NUREG/CR-0312.
18. Ruggles, A.E., 1990 Countercurrent flow limited heat flux in the high flux isotope reactor (HFIR) fuel element, ORNL/TM-9662.
19. Sudo, Y., Kaminaga, M. 1989 A CHF characteristic for downward flow in a narrow vertical rectangular channel heated from both sides, *Int. J. Multiphase Flow* **15**, 755-766.